Hydraulic Physical Modeling and Observations of a Severe Gap Wind

TIMOTHY D. FINNIGAN AND JASON A. VINE

Department of Civil Engineering, University of British Columbia, Vancouver, British Columbia, Canada

PETER L. JACKSON

Department of Geography, University of Western Ontario, London, Ontario, Canada

SUSAN E. ALLEN

Department of Oceanography, University of British Columbia, Vancouver, British Columbia, Canada

GREGORY A. LAWRENCE

Department of Civil Engineering, University of British Columbia, Vancouver, British Columbia, Canada

DOUW G. STEYN

Department of Geography, University of British Columbia, Vancouver, British Columbia, Canada

(Manuscript received 28 September, in final form 15 April 1994)

ABSTRACT

Strong gap winds in Howe Sound, British Columbia, are simulated using a small-scale physical model. Model results are presented and compared with observations recorded in Howe Sound during a severe gap wind event in December 1992. Hydraulic theory is utilized to explain along-channel variation in wind. Field observations affirm the findings of the physical modeling with both, indicating the presence and location of controls and hydraulic jumps in the wind layer. Hydraulic behavior is found to change as the synoptic pressure gradient and the flow rate increase. In particular, field results indicate two distinct hydraulic situations: one during relatively weak wind, the other, which is more strongly controlled, during the period of peak wind. An additional comparison is made with output from the computer model hydmod of Jackson and Steyn. Numerical simulations, configured for the conditions present in Howe Sound during the December 1992 event, indicate channel hydraulics (and thus spatial wind speed variation) closely resembling the physical model and field results.

1. Introduction

The Coast Mountains of western British Columbia often act as a partial barrier between differing air masses. During the winter months, an arctic outbreak can force cold air southward into the interior plateau region of British Columbia (see Fig. 1), where it may reside for several days. This air, being cold and therefore dense relative to that over the Pacific coast, is accelerated through the mountain barrier as a result of the pressure gradient established between the differing air masses. The cold air remains near the land surface, displacing the warmer air above as it flows through mountain passes and enters the coastal region. The gap winds that result in the coastal fjords can be very strong and often produce hazardous conditions.

The present paper was prompted by the work of Jackson and Steyn (1994a, 1994b; hereafter referred to as JS1 and JS2, respectively), who studied gap winds in Howe Sound, British Columbia, (see Figs. 1 and 2) using large-scale numerical modeling, field observations, and a hydraulic computer model (hydmod). These papers indicated that during strong gap wind events in Howe Sound, the low-lying layer of dense flowing air exhibits hydraulic behavior. The research described herein focuses on the hydraulics of gap wind in Howe Sound and the spatial resolution of wind in the direction of flow.

Results of a hydraulic physical model are presented and compared with observations and the hydraulic model of JS2. The field data acquired are from the outflow event in Howe Sound, which commenced on 27 December 1992 and persisted throughout the following four days, while an arctic air mass and anticyclone re-

Corresponding author address: Dr. Susan E. Allen, Dept. of Oceanography, University of British Columbia, Vancouver, British Columbia V6T 1Z4, Canada.

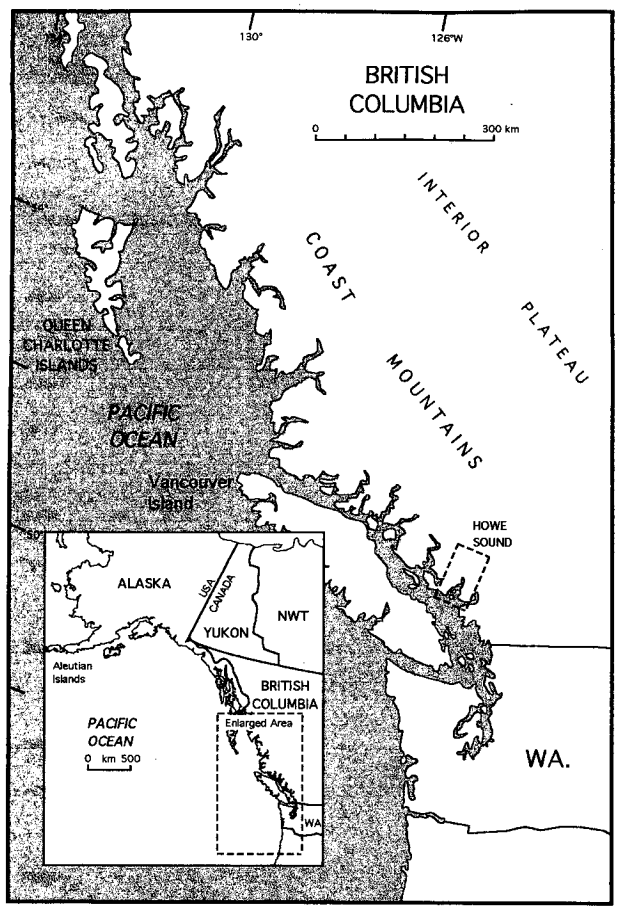

FIG. 1. Geographical location and important features of region surrounding Howe Sound.

sided in the interior of British Columbia. Channel hydraulics, predicted by the physical model studies, provided guidance in establishing the field research program.

We are able to show, by comparing field study results with model predictions, that distinct hydraulic profiles persist in Howe Sound for long periods of time during an outflow event. The term *hydraulic profile* refers to the variation in depth and densimetric Froude number (discussed below) in the along-channel direction. The identification of these hydraulic profiles allows us to specify which flow regime (sub- or supercritical) occupies specific sections of Howe Sound and thereby indicate the areas of most intense wind.

Hydraulic theory is applied to describe the along-channel variation in flow behavior in the same manner as JS2. The densimetric Froude number is used to categorize the flow as either subcritical or supercritical. Here we define the Froude number as $F = u(g'h)^{-1/2}$, where u is fluid velocity, $g' = g(\Delta\rho/\rho_0)$ reduced gravity, and h depth of the wind layer. The wind layer, having density ρ_0, is surmounted by the atmosphere above, having density $\rho_0 - \Delta\rho$, and is thus influenced by gravity g, which is effectively lowered to the value of g'. The flow is said to be subcritical if $F < 1$, critical if $F = 1$, and supercritical if $F > 1$. In open channels, the flow is controlled by channel features that determine a depth–discharge relationship (Henderson 1966). Such features (local contractions or changes in surface elevation) are called *hydraulic controls,* or simply *controls,* and the flow changes from subcritical to supercritical as it passes through them. The reader is referred to JS1 for background on gap winds in general and in Howe Sound and to JS2 for a more complete discussion of hydraulics and its applicability to gap winds.

2. Laboratory model study

Laboratory experiments aimed at modeling atmospheric flows are uncommon, especially due to recent advances in computer technology and numerical mod-

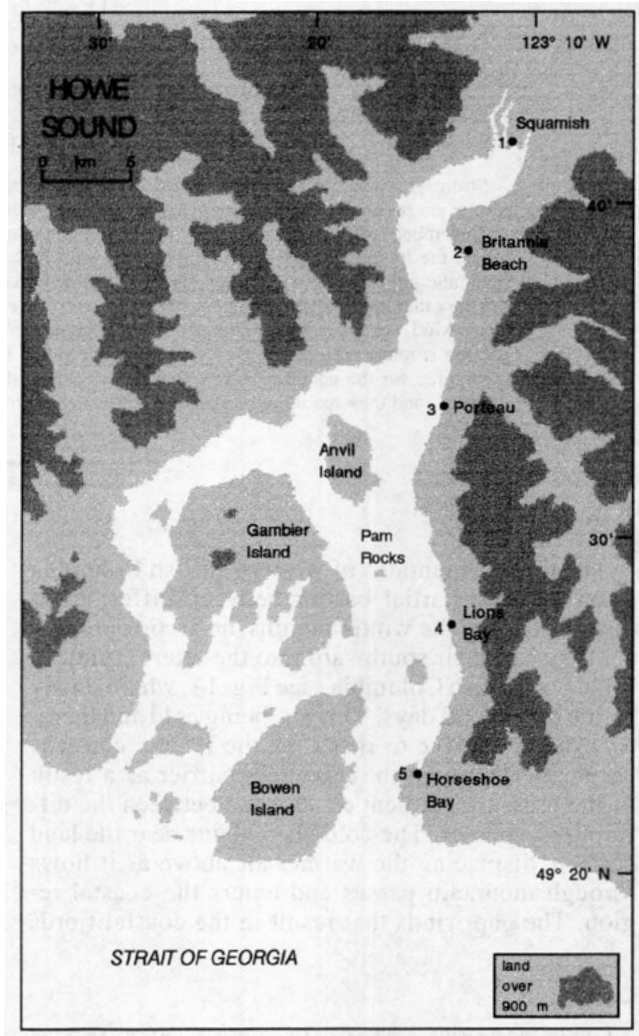

FIG. 2. Topography of Howe Sound. The locations of instruments positioned in Howe Sound are numbered 1–5 in the direction of flow.

eling. Some investigators have performed laboratory studies to verify numerical results or simply to obtain results where numerical methods are not feasible. The original work on downslope winds, which are related to gap winds, was by Long (1953), who applied hydraulic theory to the flow and reported results from a laboratory experiment simulating the "Bishop wave" phenomenon, which is thought to resemble an atmospheric hydraulic jump. A complete review of physical modeling of atmospheric flows up to 1980, which consist mostly of towing tank experiments, was done by Baines and Davies (1980). They describe how a wide range of two-layer flows, where the upper layer is essentially of infinite depth, can be accurately modeled in the lab using a single layer of fluid. More recently, Simpson and Britter (1980) conducted laboratory model experiments simulating an atmospheric mesofront. They used water to replicate the movement of air in a gravity current in calm ambient conditions and in the presence of tail- and headwinds. Simpson (1982) extended the investigation and discussed the behavior of gravity currents under varying conditions in the laboratory, atmosphere, and ocean. In the present paper, we report results from a laboratory experiment that simulated the flow of the confined wind layer in Howe Sound during an extreme gap wind event.

The physical modeling program was designed specifically to investigate the hydraulics of an extreme outflow wind in Howe Sound. This section describes the experimental arrangement, and the results are discussed in section 2b. The hydraulics of the wind layer, as predicted by the model, are presented for two model flow rates.

a. Experimental methods

In order to determine the underlying dynamics, some simplifying assumptions were made in the development of the model study program. Although some of these assumptions lead to characteristics of the model being quite different from those of the prototype (Howe Sound), the topographical aspects of the prototype that influence the hydraulics of the flow were retained.

The laboratory model system consists of a Plexiglas model channel, a 6″-wide flume, and a video camera with which to document the flow (see Fig. 3). A one-layer model was used with water representing the outflowing wind layer. Effects due to the upper atmospheric layer and mixing and friction between the layers were neglected. The experiments were performed in the hydraulics laboratory of the Department of Civil Engineering at the University of British Columbia.

Effects of the sinuosity of Howe Sound were not included in this study. Although the complicated topography of the actual channel is likely to produce an equally complicated flow, we are only interested here in the layer-averaged behavior that is governed by the basic hydraulics of the flow. This idealization permits

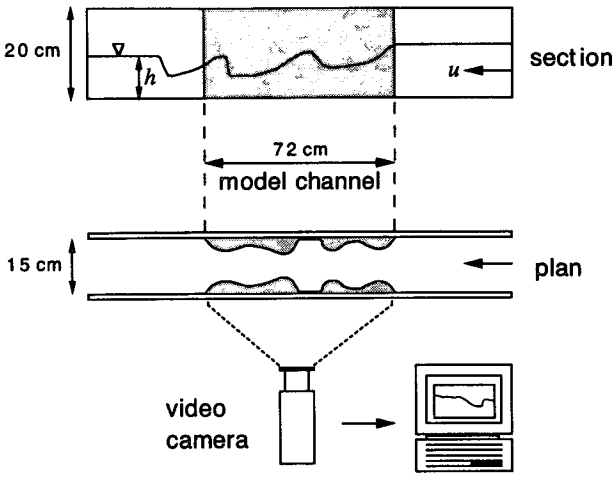

FIG. 3. Schematic drawing of experimental apparatus used for physical modeling of gap wind. The line marked with the symbol ∇ indicates a simulated water level in the vertical section.

the design of a model with a straight central axis in the flow direction across which there is symmetry (Fig. 3). A further simplification was made by assuming that the slope of the channel walls does not greatly influence the hydraulics. This assumption allowed the model to have vertical side walls. For a channel with vertical walls and flat bottom, the flow is controlled by changes in width. The depth of the wind layer during an extreme event was expected to be approximately 1000 m (Jackson 1993), so the width variation along Howe Sound was taken to be the width at an elevation of 500 m.

To accommodate the large passage between Anvil Island and the west coast of the sound (49°35′N, 123°17′W—Fig. 2), the model was simply widened out to the walls of the flume. Smaller passages between the three main islands were assumed to be insignificant relative to the main channel and were incorporated into the model in the form of widening.

The model was designed with a prototype to model horizontal length ratio of 68 000 and a vertical length ratio of 16 600. Froude number equivalence between model and prototype was used to match the flows and to scale model results to prototype dimensions.

The model was placed in the flume with the camera's viewing axis positioned perpendicular to the flow direction, as shown in Fig. 4. While being videotaped for later analysis, water was allowed to flow through the model continuously. The recorded video images were digitally processed to extract depth measurements so as to compile surface profiles of the flow. The volumetric flow rate was measured using a propeller-type flowmeter upstream of the model. This information was used to calculate the Froude number throughout the channel, determining the locations of controls and hydraulic jumps and defining the regions of sub- and supercritical flow.

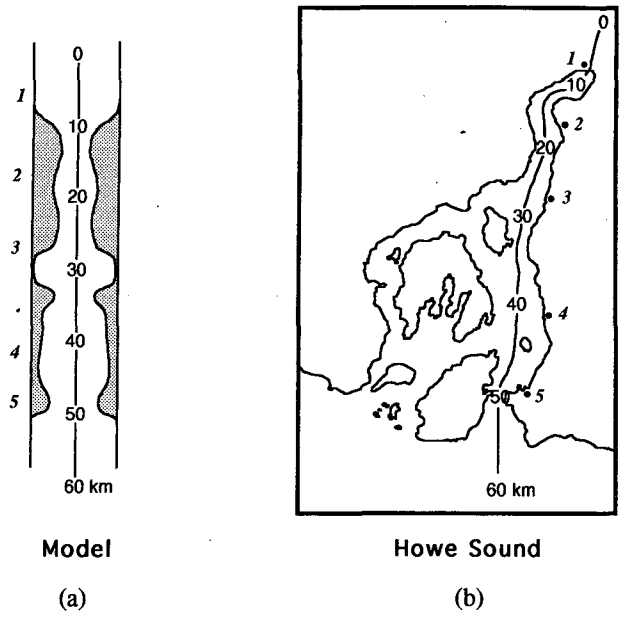

FIG. 4. Channel axis shown with respect to the model of Howe Sound (a) and Howe Sound (b). Distance increases in the direction of flow, and the field research station locations are labeled 1–5.

Uncertainty in model results can be attributed to various sources. Hydraulic theory assumes flow velocity is parallel to the channel axis and constant over cross sections in the flow. This assumption neglects boundary layers and secondary flows. The model results are obtained from measurements along the channel axis that are then assumed to be constant across the channel width. In some parts of the channel, depth varied slightly across the channel width, indicating velocities not parallel with the channel axis. As well, the Reynolds number of the prototype flow is generally several orders of magnitude larger than that of the model flows, which does not affect the results as far as hydraulic properties are concerned but may produce different velocity distributions.

b. Results

Model runs were performed for several flow rates. The lowest flow rates did not force any channel features to act as hydraulic controls, leaving the flow subcritical throughout the channel. As flow rates were increased, certain features of the channel began to control the flow. The hydraulic profile changed when critical flow was achieved at a particular location in the channel [i.e., $u = (g'h)^{1/2}$].

A curvilinear channel axis through Howe Sound is shown along with its straightened model counterpart in Fig. 4. In each of the figures (Figs. 5 and 6) that present the spatial variation of quantities along Howe Sound, the length scale represents the distance along the channel axis in the direction of flow. Results from the physical modeling, field experiment, and hydmod (JS2) output appear together in Figs. 5 and 6 in order to facilitate direct comparison. Each set of results is introduced separately before being compared in section 4.

1) RESULTS FOR FLOW RATE *A*

For a model flow rate of 0.032 $m^3 s^{-1}$ (hereafter referred to as flow rate *A*), the predicted wind-layer elevation (or depth) is shown in Fig. 5a. The horizontal model length scale has been converted to that of the prototype to allow for direct comparison with field measurements. Flow is from right to left, with the 0-km location being the upstream end of the channel and the 60-km location being downstream of the channel terminus. Results are presented this way to facilitate direct comparison with hydmod output that is generated in this format (see JS2). Wind speed variations along the channel are shown in Fig. 5b, where high wind speeds coincide with regions of supercritical flow. Figure 5c shows the Froude number as it varies along the model channel for flow rate *A*.

Upon entering the channel, flow is accelerated by the contracting walls and reaches the critical point ($F = 1$)

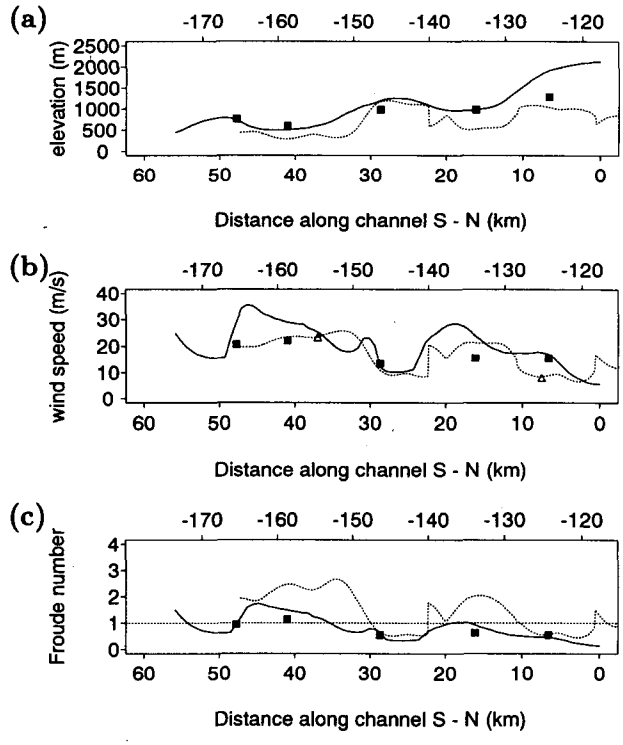

FIG. 5. (a) Depth, (b) wind speed, and (c) Froude number along Howe Sound: as predicted by the physical model for flow rate *A* (solid line); as measured during the December 1992 outflow event for period 1 (solid squares—field data, open triangles—observed 10-m wind); and as produced by the numerical model hydmod (dashed line) for period 1. Flow is from right to left, and a point of hydraulic control exists wherever the $F = 1$ line is crossed from less than 1 to greater than 1 (i.e., sub- to supercritical flow).

at about 17 km. It appears that supercritical flow exists for a short distance beyond the control section before a sudden expansion (22 km) in the channel induces a hydraulic jump, transforming the flow from supercritical to subcritical. The flow again becomes supercritical near 35 km following the contraction imposed by Anvil and Gambier Islands. This controlling feature is much stronger than the first, as is evident in the high values of F. Another expansion beyond Gambier Island (40 km) forces the occurrence of a hydraulic jump at about 48 km. The narrow passage between Bowen Island (50 km) and the east side of the channel forces a transition to supercritical flow that extends beyond the channel terminus where a hydraulic jump reconnects the flow with subcritical conditions in the Strait of Georgia.

2) RESULTS FOR FLOW RATE B

Results for a higher model flow rate of 0.043 $m^3 s^{-1}$ (hereafter referred to as flow rate B) appear in Fig. 6. An increase in flow rate from A to B produced similar results to those explained above but with some notable differences. The same features act to control the flow, but the hydraulic profile is expectedly characteristic of a stronger flow. Supercritical flow is first reached farther upstream (14 km) and extends for several kilometers before the expansion near 22 km induces a hydraulic jump near 27 km. The position of this jump is farther downstream than that for flow rate A. The higher flow rate has extended the supercritical flow region here by moving the critical point upstream and the hydraulic jump downstream.

The flow rate increase from A to B does not seem to enlarge the supercritical region between 35 and 48 km. It is likely that the positions of the control and subsequent hydraulic jump that encompass this region are fixed by the channel topography (for flow rates A and B) and essentially confine the supercritical region. The flow exits the channel in much the same way as for flow rate A.

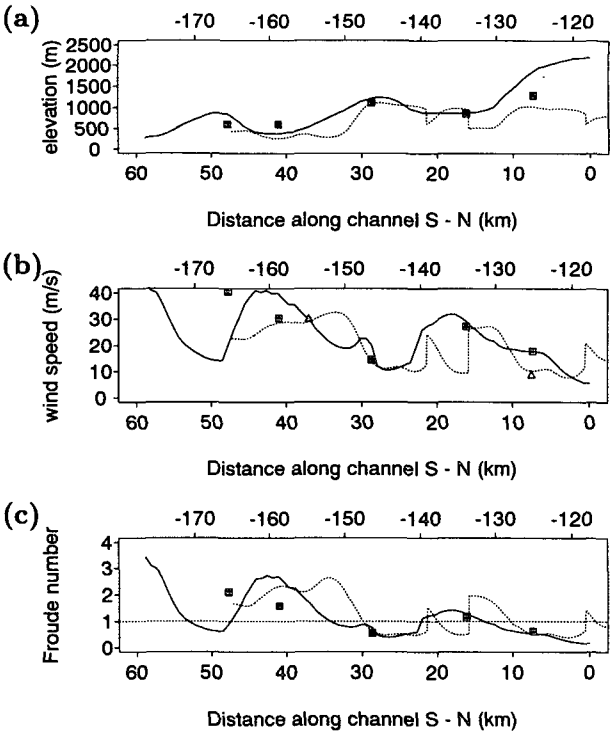

FIG. 6. (a) Depth, (b) wind speed, and (c) Froude number along Howe Sound: as predicted by the physical model for flow rate B (solid line); as measured during the December 1992 outflow event for period 2 (solid squares—field data, open triangles—observed 10-m wind); and as produced by the numerical model hydmod (dashed line) for period 2. Flow is from right to left.

3. Field program

a. Synoptic weather conditions for the December 1992 event in Howe Sound

The evolution of synoptic-scale weather patterns creates the atmospheric boundary conditions within which gap winds occur. The synoptic conditions in the December 1992 case are typical of other gap wind cases (Jackson 1993). An upper-level ridge, lying north–south across the Aleutian Islands (Fig. 1), increased in amplitude during 26–27 December 1992. Meanwhile, an upper-level cold low and an associated 998-mb sea level low developed in a trough to the east and moved southward down the British Columbia coast to a quasi-stationary position 900 km southwest of Vancouver Island by 0400 LST 27 December. This pattern resulted in east to northeasterly flow aloft over the coastal zone. Linked with the upper-level ridge, a 1060-mb surface high pressure zone, associated with very cold arctic air, formed over Alaska and moved to a quasi-stationary position over central Yukon Territory by 0400 LST 27 December. Associated with these developments, an arctic front moved southwards across Howe Sound during the day on 28 December. Behind the arctic front, a zone of very large horizontal sea level pressure gradient, oriented perpendicular to the coast, resulted in strong low-level gap winds through the valleys and fjords dissecting the coast range. The strong pressure gradient and resulting winds began to weaken after 29 December, when the upper-level ridge–trough pattern decreased in amplitude, the Yukon high moved southeastwards in British Columbia, but weakened, and the arctic front moved farther offshore.

b. Field experiment

To further document the existence of hydraulic controls in Howe Sound and attempt to identify their locations, a field investigation was undertaken. The field research program was initiated at the beginning of the 1992/93 winter season, and one extreme outflow event occurred in December 1992. Measured pressure vari-

ations between selected sea level stations along the sound during the event show distinct along-channel hydraulic profiles. The interpretation of the pressure data allows determination of controls in the channel.

Surface pressures during the strong outflow event that commenced on 27 December 1992 were recorded by microbarographs placed at five stations along Howe Sound. The pressure variation with time, recorded at each location, indicates the relative thickness of the outflowing layer at each station. Pressure differences between stations indicate a change in depth of the outflowing layer. The mean pressure due to the entire atmosphere is assumed to be approximately equal at all stations (which lie within a 50-km range) before the onset of outflow. When an outflow event occurs, the added pressure, due to denser air in the outflow layer, varies between stations, indicating changes in layer depth along the channel.

Jackson (1993) shows that the flow is confined, to some degree, to the main eastern channel of Howe Sound, with Bowen Island, Gambier Island, and Anvil Island forming a partial barrier to the flow (see Fig. 2). For this reason, instruments were placed along the eastern shore of the main channel. An effort was made to place the instruments at locations on the shore as close as possible to the central axis of the channel. Since the model (and hydraulics in general) produce cross-sectionally averaged quantities, the field results are assumed to be representative of the cross-sectional average.

The locations of the recording stations were chosen strategically to coincide with regions between hydraulic control sections in the sound. The results of the physical model were used to predict the points of hydraulic control and indicate roughly where to position the instruments. The instrument locations relative to the model are indicated in Fig. 4a as points numbered 1–5 (also shown on Fig. 2). These locations are situated between control sections in the model and correspond to actual locations in Howe Sound where the instruments were placed (Fig. 4b). A difference in recorded pressure across a control section during an outflow event would indicate a change in depth (between those stations) and a possible transition between flow regimes. The transition may occur either smoothly from sub- to supercritical flow or rapidly as a hydraulic jump from super- to subcritical. A decrease in pressure in the direction of flow would indicate the former, while an increase would indicate the latter. This information leads to the determination of which flow regime occurs at each of the five field stations.

c. *Field data interpretation*

Figure 7 is a composite of the pressure recordings of all five stations over a period of 9.5 days, where hour 0 coincides with 0000 LST 25 December 1992. Each pressure trace corresponds to one of the stations shown in Fig. 4. At each station, the pressure initially varies only with the large-scale synoptic field. This variation is seen in Fig. 7 up until about hour 52. On 27 December at about hour 60, winds and relative pressure deviation among stations increased in the channel. These pressure differences represent depth changes in the gap wind that develop as the flow accelerates and decelerates through the channel topography. The flow is unsteady, with the pressure differences (depth differences) increasing during the onset and varying through the duration of the outflow event. Finally, as the wind subsides (hour 180), the pressure differences among stations decrease and coincide with the mean regional pressure.

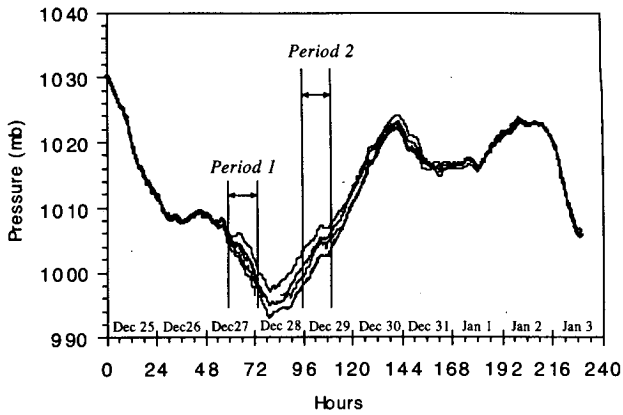

FIG. 7. Composite chart of atmospheric pressures recorded at five stations in Howe Sound over a 9-day period. Strong gap winds occurred from 27 December to 1 January.

Data acquired from an automatic weather station, located at Pam Rocks (see Fig. 2) in the middle of the channel near station 4, were used to confirm the pressures recorded at station 4. As well as pressure, the Pam Rocks station recorded wind velocity and temperature. From the velocity, temperature in the wind layer, temperature in the atmosphere above the wind layer (estimated from recorded temperatures just before onset of outflow), and relative pressure information, it is possible to estimate the absolute depth of the wind layer at station 4. The calculations involved in this estimate are outlined in appendix A. Converting the relative pressure at each station to relative depth (assuming hydrostatic pressure variation), and using the known depth at station 4, the depths at all stations can be determined at any time. From the information at station 4, the volumetric flow rate in the wind layer can be calculated. By estimating the average width of the channel at each station from topographic maps (width at half depth) and assuming the volumetric flow rate to be constant throughout the channel, the Froude number F can be determined at each station at any particular time during the outflow event (see appendix A for details on the calculation). If a change in depth between

stations is accompanied by a change in flow state (indicated by a change in F from greater than 1 to less than 1 or vice versa), then it is assumed that a control or hydraulic jump exists between the stations.

Through the course of the 4-day outflow, two distinct along-channel hydraulic profiles are evident. The first lasts from the onset of the outflow until the flow is well established. The second, being forced by a higher horizontal pressure gradient and characterized by an increased flow rate, persists for approximately 12 h before the wind begins to subside. The period of time occupied by each is indicated on Fig. 7 as period 1 and period 2, respectively. Both hydraulic profiles are described below.

The acquisition of the field data and the process by which the acquired data were transformed into the final results introduce some uncertainty. The instruments contribute some error to the raw data (±0.25 h, ±0.2 mb), but the main sources of overall error are due to the process of approximating channel dimensions and averaging the results over time.

1) Results for period 1

Following the initial increase, the gap wind layer develops a steady hydraulic profile that persists for 12 h: from hour 60 to hour 72 during the day of 27 December. This time frame is indicated in Fig. 7 as period 1. In order to more clearly see the changes between stations, the field results are shown again in Fig. 8, where the difference in pressure from station 1 (P_1) is plotted for each station. For station 1, the difference is of course zero, resulting in a straight line. During period 1 (Fig. 8a), the pressure and hence depth decreases between stations 1 and 2 and seems to be the same at stations 2 and 3. Beyond station 3, the pressure drops substantially at station 4 before increasing again at station 5.

The winds during period 1 are thought to be associated with a transient stage in the outflow event. This stage represents the onset of the flow and is characterized by lighter winds, with stronger winds occurring once the flow is fully established. This low-flow-rate stage of the outflow corresponds with the low-flow-rate run (A) of the model results. The average depth, wind speed, and Froude number calculated for this stage of the flow are plotted (as solid square points at each of the five stations), along with the results for the physical model flow rate A in Fig. 5.

Between hour 72 and hour 88, data at stations 3 and 4 were lost due to instrument failures.

2) Results for period 2

As the winds increased during the evening of 28 December, the along-channel hydraulic profile changed to a new state. This is indicated as period 2 in Fig. 7 and Fig. 8. Referring to Fig. 8b, the pressure now drops

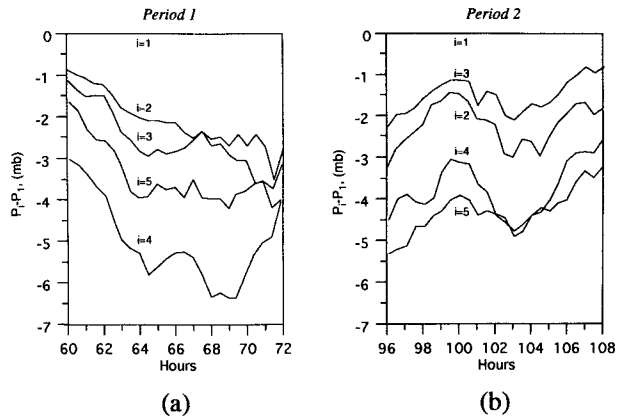

FIG. 8. Relative pressures, with respect to that at station 1 (P_1), at each of the five field stations in Howe Sound ($i = 1-5$) for (a) period 1 and (b) period 2.

substantially between stations 1 and 2 before increasing again at station 3. Following station 3, the pressure drops again between stations 3 and 4 and now remains low at station 5.

This period of the event is characterized by higher winds and more closely resembles the physical model results for the higher flow rate (B). The average depth, wind speed, and Froude numbers for this period are plotted (as solid square points at each of the five stations) on Fig. 6, along with the model results for flow rate B.

4. Comparison of physical model, hydmod, and field results

Since the field results only indicate the conditions at five points along the channel, it is possible that some aspects of the hydraulics are not revealed by them. By comparing the field results directly with hydraulically similar model results (i.e., approximately equivalent Froude numbers), however, the conditions throughout the channel can be inferred.

a. Period 1 (flow rate A)

During the onset of an extreme gap wind event, before the winds have reached full strength, the hydraulics of the wind in the main channel of Howe Sound are expected to resemble what is shown in Fig. 5. The field results confirm model predictions of subcritical flow at the channel entrance (station 1). The flow accelerates as it progresses downstream toward station 2, as indicated by increasing Froude number and decreasing depth. Field results indicate that the flow is subcritical at stations 2 and 3, as do physical model results. The model indicates that a control and subsequent hydraulic jump can develop between stations 2 and 3 if the flow rate is high enough. The resulting region of supercritical flow between stations 2 and 3 will expand

upstream with increasing flow rate (as will be discussed below) and eventually encompass station 2. The expansion in the channel near 25 km (just upstream of Anvil Island) results in subcritical flow limiting the extent of the supercritical region upstream.

Beyond station 3, the flow is accelerated through the contraction imposed by Anvil Island and passes through a control point near 35 km before reverting to subcritical flow in a hydraulic jump near 48 km. The physical model and field results agree in this region, although the Froude number at station 4 is less than that predicted by the model. Substantial error associated with the estimation of Froude numbers from field results (estimation of average depth, width, and velocity) and modeling inadequacies can account for this discrepancy. The lower Froude number reported from the field results may be due to the existence of the side channels between the islands that were ignored in the model. Despite minor discrepancies, the model and field results confirm the general hydraulic behavior in this region. The supercritical region that reaches its maximum expanse (at low flow rates) between 35 and 48 km is confined on both ends by regions of subcritical flow.

Beyond station 5, no field results are available. The model predicts that downstream of station 5, the flow is controlled again as it passes through the contraction between Bowen Island and the protrusion on the east side of the channel (Fig. 2). From field results, a simple calculation shows that the width reduction between station 5 and this point may force transition (see appendix B for the calculation). The flow exits the channel supercritically and must then reconnect to subcritical conditions in the Strait of Georgia through a hydraulic jump downstream. This jump was observed downstream of the model in the flume.

b. *Period 2 (flow rate B)*

For the higher flow rate some of the hydraulic characteristics of the model flow are readily confirmed by the field results, while others require some interpretation. Throughout most of the channel, the situation is much the same as described above. Flow enters the channel subcritically and is accelerated (Fig. 6). With increased flow rate, however, the control that was between stations 2 and 3 in the above discussion has advanced upstream beyond station 2. The model now indicates supercritical flow at station 2 and the field results confirm this. The flow returns to subcritical before station 3, as the expansion (25 km) forces transition through a hydraulic jump.

As is the case for the lower flow rate, the flow is controlled near Anvil Island (35 km) before reaching station 4. Through the region spanned by stations 4 and 5, the model and field results differ in some respects. The field results indicate supercritical flow at station 5, whereas the model results are much the same as for the lower flow rate discussed above: subcritical flow (although near critical) at station 5. It is possible that the model strongly confines the region of supercritical flow upstream of station 5, while in reality, the hydraulic jump (Fig. 6, 47 km) may be washed downstream and possibly out of the channel. The extension downstream of this supercritical region would explain the findings at station 5.

c. *Further comparison with hydmod output and observed wind speed*

For further comparison, the numerical hydraulic model hydmod was run for the conditions in Howe Sound during period 1 and period 2. The average along-channel synoptic pressure gradient dp/dx for each period was calculated from direct observations at two government stations (Pemberton, 67 km upstream from Squamish and Pam Rocks). Table 1 lists the values of each input parameter for both periods. All input data are from observed values.

The hydmod results appear as a dashed line along with the physical model and field results in Figs. 5 and 6, where the scale across the top corresponds to the convention used for RAMS and hydmod results in JS1 and JS2. Near the channel entrance, the supercritical flow is predicted to jump to subcritical. Although not within the range of the physical model or field results, this jump may actually occur with the wind descending the mountain slope upstream of Squamish in the supercritical regime before entering a flat expansion that could induce a hydraulic jump. Referring to Figs. 5 and 6, hydmod predicts that the channel hydraulics are governed by the same controls identified by the physical modeling and field observations. The two models show slight differences in the exact location of these controls and the ensuing hydraulic jumps. This is due to the vastly different nature of the two models and the different representations of channel topography and friction coefficients (among other things) that each relies on. One notable difference is the large supercritical region predicted by hydmod between 10 and 23 km in Fig. 5, which does not appear in the physical model results for flow rate *A*. In Fig. 6, hydmod indicates the

TABLE 1. Values of parameters as observed during period 1 and period 2 that were used in hydmod comparisons.

Input variable	Period 1	Period 2
Synoptic pressure gradient dp/dx (Pa m^{-1})	0.0121	0.0168
Initial height h_s (m)	1200	1200
Total discharge Q (m^2 s^{-1})	6.5×10^7	7.4×10^7
Lower potential temp. θ_1 (K)	272	265
Upper potential temp. θ_2 (K)	281	281
Drag coefficient C	0.02 land 0.01 water	0.02 land 0.01 water

flow is controlled near 10 km, but passes through a hydraulic jump and subsequent control before reverting to subcritical flow near 27 km. This additional control and jump is not predicted by the physical model and cannot be detected by the field measurements. Upstream depths differ substantially between the two models, which is likely due to each models deficiency in simulating the upstream boundary conditions. The physical model appears to overestimate the upstream depth for both flows (Figs. 5 and 6). Despite the differences, the hydmod results serve to confirm the existence of the hydraulic profiles as predicted by the physical model and as suggested by field observations.

Directly observed wind speeds at two weather stations (Squamish town at 8 km and Pam Rocks at 38 km) provided additional information, which appears in Figs. 5b and 6b as two discrete open triangles in each. The upstream values from Squamish town were calculated by averaging the hourly mean observations over the 12 h represented by each figure (i.e., period 1 and period 2). These values may be slightly lower than the mean-layer flow speed because of the influence of boundary layer effects on 10-m wind. The downstream values from Pam Rocks are calculated by arithmetic averaging of peak hourly gusts that more closely represent the mean-layer flow speed. The correspondence with model results (physical and numerical) is good at the downstream point for both periods. Due to the uncertainty associated with the upstream point, it is difficult to conclude which model better predicts the wind speed at that location.

5. Discussion and conclusions

Physical modeling of gap winds in Howe Sound, followed by field measurements recorded during an actual outflow event, led to an understanding of the hydraulic behavior of the wind layer for two distinct flow rates: one representing lighter winds typical of the onset period of an outflow event, the other representing the fully established flow. Comparison of the physical model and field results confirmed the model findings at specific points and thereby allowed the inference of prototype behavior from model predictions at other locations in the channel. For the lower flow rate (period 1, flow rate A), short regions of supercritical flow were observed. With an increased flow rate (period 2, flow rate B), these regions were observed to expand and occupy more of the channel. In some cases, fixed control points limited the expansion of the supercritical regions, effectively confining them between regions of subcritical flow.

The two modeling exercises serve to reinforce the findings of the observational program and allow the specification of which hydraulic regime is prevalent at locations along Howe Sound during a gap wind event. Supercritical flow and corresponding extreme wind conditions are defined in Figs. 5 and 6. Model results show some deviation from field results for fully established flow. Insufficient similarity between the physical model and the prototype near the channel terminus and beyond may explain the fixed control that exists in the model but is not observed in the field. Further physical modeling, incorporating improved geometric and dynamic similarity, will allow a more extensive analysis of the hydraulics of gap winds, not only along the channel but across it.

Acknowledgments. The authors wish to thank Sewell's Marina (Horseshoe Bay), Lion's Bay Marina, the Cunneyworths (Porteau Cove), Britannia Beach Arts and Crafts, and the Squamish Terminals for allowing microbarographs to be stationed on their premises during December 1992 and January 1993. Pacific Region of the Atmospheric Environment Service provided the supplemental field data from Pam Rocks. The research was supported by grants from the Atmospheric Environment Service of Environment Canada and the Natural Science and Engineering Research Council.

APPENDIX A

Calculation of Froude Number, Wind Layer Depth, and Velocity at Each Field Station

a. Description of the method

In order to examine the hydraulics of the wind layer in Howe Sound during the December 1992 event, it was necessary to convert the recorded absolute pressures and relative pressure changes along the channel to absolute layer depths. The absolute layer depth at one field station had to be determined in order to use the recorded relative pressure change between each station (assuming hydrostatic pressure distribution) to calculate absolute depth at each station.

The Atmospheric Environment Service's (AES) weather station at Pam Rocks is situated near our recording station at Lion's Bay (station 4). Hourly pressure data acquired at Pam Rocks during the event were used to confirm our data at station 4. As well as pressure, the Pam Rocks station also records wind speed and air temperature. These data, along with our pressure data at stations 4 and downstream at station 5, were used to estimate the absolute layer depth at station 4 and therefore at all the stations.

The procedure involves the assumption that during period 1 of the event, the increase in pressure between stations 4 and 5 is due to the presence of a hydraulic jump. The steady pressure difference between the stations of approximately 1 mb during period 1 (Fig. 8a) validates this assumption.

b. Method of solution

The hydraulic jump equation, as described in Henderson (1966) and expressed in terms of the upstream conditions, can be used to predict the depth of flow just

downstream of a hydraulic jump. In its usual form, which assumes the channel is rectangular in section and neglects friction and synoptic pressure gradients, the equation appears as

$$\frac{h_2}{h_1} = \frac{1}{2}[(1 + 8F_1^2)^{1/2} - 1], \qquad \text{(A1)}$$

where F_1 is the Froude number upstream of the jump, and h_1 and h_2 are the upstream and downstream depths, respectively. Expressing F_1^2 as $u_1^2/g'h_1$ and h_2 as $h_1 + \Delta h$, where Δh represents the change in depth across the hydraulic jump, and solving (A1) explicitly for h_1, leads to the following form of the hydraulic jump equation:

$$h_1 = \frac{1}{4}\left\{-\left(3\Delta h - 2\frac{u_1^2}{g'}\right) + \left[\left(3\Delta h - 2\frac{u_1^2}{g'}\right)^2 - 8\Delta h^2\right]^{1/2}\right\}, \qquad \text{(A2)}$$

where the reduced gravity,

$$g' = g\frac{(\rho_1 - \rho_2)}{\rho_1}, \qquad \text{(A3)}$$

is a function of the upper- and lower-layer densities that we will call ρ_2 and ρ_1, respectively. Equation (A2) yields the depth of flow upstream of a hydraulic jump in terms of the upstream fluid velocity u_1, the depth change across the jump Δh, and the reduced gravity g'.

The density can be determined from the ideal equation of state,

$$\rho = \frac{P}{RT}, \qquad \text{(A4)}$$

where P is the pressure, T is the temperature in the particular layer, and R is the gas constant for air. The data from Pam Rocks provide the temperature T_1 in the lower layer, whereas the temperature in the upper layer T_2 is approximated by surface temperature readings taken shortly before the onset of the event (before a lower layer of intruding cold air occupied the region). Only pressure in each layer is then needed to determine the densities and therefore the reduced gravity.

The data at station 4 gives us the pressure at the ground surface that, considering the relatively small vertical extent of the lower layer, approximates the pressure P_1 in the lower layer. Pressure in the upper layer (near the interface) is determined, assuming the pressure varies hydrostatically, from

$$P_1 = P_2 - \rho_1 g' h_1. \qquad \text{(A5)}$$

This relation involves quantities described by the previous equations, which in turn rely on it.

The only remaining unknown in (A2) is Δh. This quantity is determined from the relative pressure change across a hydraulic jump ΔP, as recorded between stations 4 and 5, that is,

$$\Delta h = \frac{\Delta P}{\rho_1 g'}. \qquad \text{(A6)}$$

Now all quantities in (A2) have been determined, and the system consisting of (A2), (A3), (A4), (A5) and (A6) can be solved iteritively for h_1.

c. Calculation of layer depth, Froude number, and velocity at each station

Using the hydrostatic equation in the form of (A6), the layer depths at each station are found from the relative pressure data once the absolute depth at station 4 is determined.

The Froude number can be expressed in terms of the flow rate per unit width q rather than the velocity, in the following manner:

$$F^2 = \frac{q^2}{g'h^3}. \qquad \text{(A7)}$$

The total flow rate, $Q = qb = uhb$, where b is the average width of the channel calculated at station 4 using the known velocity, depth, and width there, is assumed constant throughout the channel. Since the average channel width b can be measured from topographic maps and the value of Q is known at each station location, the value of q is also known. This, coupled with the known depth at each station, gives the Froude number and the velocity at each station.

APPENDIX B

Calculation of Transition to Supercritical Flow Downstream of Station 5 for Period 1

For the model results with flow rate A, the flow is predicted to transit from sub- to supercritical downstream of the location corresponding to the field station 5. The field results indicate subcritical flow at station 5 ($F = 0.9$), but no results are available downstream to directly confirm the model-predicted transition.

A simple calculation, using the known conditions at station 5 and the extent of further contraction in the channel beyond station 5, reveals that transition is likely immediately downstream as predicted by the model. Here we use the concept of specific energy, from hydraulic theory, to relate the flow between station 5 and the point of minimum channel width just downstream. Specific energy may be defined at a particular location in the flow by

$$E = h + \frac{q^2}{2g'h^2}, \qquad \text{(B1)}$$

where synoptic pressure gradient is neglected, and h is

the depth of flow, q the flow rate per unit width, and g' the reduced gravity. Neglecting frictional losses between station 5 (which we will refer to as location 1) and the point of minimum width (location 2), the specific energy remains constant between the two points.

The specific energy at 1 is calculated to be E_1 = 1010 m, which is also the value at 2. The average channel width at 2 is reduced to approximately 60% of that at 1.

Therefore, the flow rate per unit width at 2 is

$$q_2 = \frac{q_1}{0.6} = 22 \times 10^3 \text{ m}^2 \text{ s}^{-1}, \qquad \text{(B2)}$$

where the numerical values are determined from the calculations described in appendix A. Inserting these values into (B1) for position 2 and solving the resulting cubic equation for h_2 yields two alternative depths at position 2: one for subcritical flow and one for supercritical flow (see Henderson 1966). The root corresponding to the supercritical depth of flow for the equivalent specific energy at 1 has the value y_2 = 673 m, which is lower than the depth at 1, y_1 = 763 m. This state may be reached if the flow passes through the point of minimum specific energy (critical point). We have now determined both q_2 and y_2, which, using (A7), gives the Froude number at location 2. The value obtained is F_2 = 1.6, indicating supercritical flow at that location.

The above calculation, from the field results, affirms the model prediction that a transition may occur from subcritical flow at station 5 to supercritical flow downstream before the channel terminus.

REFERENCES

Baines, P. G., and P. A. Davies, 1980: Laboratory studies of topographic effects in rotating and/or stratified fluids. *Orographic Effects in Planetary Flows,* chapter 8. GARP Publication no. 23, WMO/ICSU, 233–299.

Henderson, F. M., 1966: *Open Channel Flow.* Macmillan, 69 pp.

Jackson, P. L., 1993: Gap winds in a fjord: Howe Sound, British Columbia. University of British Columbia, Ph.D. thesis.

——, and D. G. Steyn, 1994a: Gap winds in a fjord. Part I: Observations and numerical simulation. *Mon. Wea. Rev.,* **122,** 2645–2665.

——, and ——, 1994b: Gap winds in a fjord. Part II: Hydraulic analog. *Mon. Wea. Rev.,* **122,** 2666–2676.

Long, R. R., 1953: A laboratory model resembling the "Bishop-wave" phenomenon. *Bull. Amer. Meteor. Soc.,* **34,** 205–211.

Simpson, J. E., 1982: Gravity currents in the laboratory, atmosphere, and ocean. *Ann. Rev. Fluid Mech.,* **14,** 213–234.

——, and R. E. Britter, 1980: A laboratory model of an atmospheric mesofront. *Quart. J. Roy. Meteor. Soc.,* **106,** 485–500.